25. Burkart, M. W. & Read, T. A. Diffusionless phase change in the indium–thallium system. *Trans. AIME* **197,** 1516–1523 (1953).
26. Basinski, Z. S. & Christian, J. W. Cystallography of deformation by twin boundary movement in indium–thallium alloys. *Acta Metall.* **2,** 101–116 (1954).
27. Zener, C. Stress induced preferential orientation of pairs of solute atoms in metallic solid solution. *Phys. Rev.* **71,** 34–38 (1947).
28. Birkenbeil, H. J. & Cahn, R. W. Induced magnetic anisotropy created by magnetic and stress annealing of iron–aluminium alloys. *Proc. Phys. Soc.* **79,** 831–847 (1962).
29. Miyazaki, S. & Otsuka, K. in *Shape Memory Alloys* (ed. Funakubo, H.) 116–175 (Gordon and Breach, New York, 1987).

Acknowledgements. We thank T. Suzuki, T. Ohba, H. Horiuchi, M. Kogachi and Y. Murakami for helpful discussions and critical reading the manuscript; T. Ishii for technical assistance; and T. Ohba for allowing us to use his published diffraction data. The work was supported by a Grant-in-Aid for Scientific Research on Priority Area of Phase Transformations (1997–1999) from the Ministry of Education, Science and Culture of Japan. X.R. is a recipient of a JSPS Fellowship.

Correspondence and requests for materials should be addressed to K.O. (e-mail: otsuka@mat.ims.Tsukuba.ac.jp).

Bending and buckling of carbon nanotubes under large strain

M. R. Falvo*, G. J. Clary†, R. M. Taylor II†, V. Chi†, F. P. Brooks Jr†, S. Washburn* & R. Superfine*

** Department of Physics and Astronomy, †Department of Computer Science, University of North Carolina, Chapel Hill, North Carolina 27599, USA*

The curling of a graphitic sheet to form carbon nanotubes[1] produces a class of materials that seem to have extraordinary electrical and mechanical properties[2]. In particular, the high elastic modulus of the graphite sheets means that the nanotubes might be stiffer and stronger than any other known material[3–5], with beneficial consequences for their application in composite bulk materials and as individual elements of nanometre-scale devices and sensors[6]. The mechanical properties are predicted to be sensitive to details of their structure and to the presence of defects[7], which means that measurements on individual nanotubes are essential to establish these properties. Here we show that multiwalled carbon nanotubes can be bent repeatedly through large angles using the tip of an atomic force microscope, without undergoing catastrophic failure. We observe a range of responses to this high-strain deformation, which together suggest that nanotubes are remarkably flexible and resilient.

Two mechanical properties of a material are of principal interest here: the small-strain elastic modulus and the material strength. The basal-plane elastic modulus of graphite, the largest of any known material, confers on the nanotube its predicted extraordinary stiffness[3,4,24]. These expectations are consistent with reports of transmission electron microscope (TEM) measurements taken in the small-strain limit[5], and atomic force microscope (AFM) measurements which were extended beyond the linear elastic regime[8]. Although the high stiffness is predicted to provide an improvement over existing materials, it is the nanotube's unusual strength which is its most distinguishing property. The unusual strength arises from the high stiffness, expected to be consistent with the modulus of graphite, combined with extraordinary flexibility and resistance to fracture. It is this latter feature which will distinguish nanotubes from graphitic fibres as an engineering material. Two theoretical approaches to understanding and predicting the large-strain behaviour of carbon nanotubes are atomistic molecular-dynamics simulations and continuum mechanics. The remarkable correspondence between the two approaches and TEM observations has been appreciated recently in the case of the smallest single- and double-wall tubes under flexural strains which produce buckling deformations[9]. Large multiwalled nanotubes (MWNTs) present challenges to both theoretical approaches in that molecular-dynamics simulations are limited in the size of the system that can be modelled, and continuum mechanics has been most successful in the thin-shell limit.

Knowledge of the large-strain behaviour of carbon nanotubes relies largely on the TEM observations of as-deposited, small-diameter tubes. Typically, many small kinks are seen on the compressed side of an otherwise smooth bend in a MWNT[10,11]; molecular-dynamics simulations predict this kinking to be reversible even under very severe bending[12]. This is consistent with indirect evidence of reversible buckling of a carbon nanotube while attached to an AFM probe[6]. This indicates a fibre of unusual strength. Until now, experimental evidence of the structure of bent nanotubes has relied largely on finding nanotubes which have been bent either during the deposition procedure or through the distortion of the substrate[13,14]. Ideally, experiments should be performed where the full history of the strain, including the initial condition of the tube and the reversibility of the structure, is known. Using a unique interface for atomic force microscopes, we have performed intricate bending of MWNTs to large strains.

Samples were prepared by solvent evaporation on mica substrates of an ethanol solution of raw carbon soot (produced from the carbon-arc technique[15]). The carbon nanotubes were imaged and manipulated under ambient conditions. The 'Nanomanipulator' AFM system, designed for manipulation, comprises an advanced visual interface, teleoperation capabilities for manual control of the AFM tip and tactile presentation of the AFM data (Discoverer, Topometrix Inc., Santa Clara, CA)[16,17]. Initially, the tubes are straight with no apparent structural defects. The AFM tip is used to apply lateral stresses at locations along the tube to produce translations and bends. The friction between the tube and the substrate pins the tube in its strained configuration for imaging. On some samples, however, the tube/substrate friction is too low to maintain the highly strained nanotube, and relaxation of the tube is observed during AFM imaging.

A carbon nanotube, pinned at one end by carbon debris, was bent into many configurations. The inset of Fig. 1a shows the tube in its original adsorbed position and orientation. The abrupt vertical step on the left side of the tube was used as a reference mark ($s = 0$, where s is the measured distance along the tube centre line) for feature locations. The nanotube was taken through a series of 20 distinct manipulations, alternately bending and straightening the tube at various points. We present images from this sequence to highlight specific features (Fig. 1a–d). Along with AFM topographic data, we also show the tube height along the tube's centre as determined by the cores method[18,19], along with the calculated curvature (Fig. 1e–h). We will refer to raised points on the tube as 'buckles', consistent with the increase in height expected from the collapse of a shell in response to bending. We observe two behaviours in this sequence: small, regularly distributed buckles at regions of small curvature and large deformation at high curvatures.

We focus first on the regularly spaced buckles occurring in the more gradually bent region (Fig. 1a, lower right). Figure 1b and c shows the tube as it is bent in opposite directions. The location of the buckles has shifted dramatically, with the buckles of Fig. 1c appearing in regions which had been featureless, and the buckles of Fig. 1b largely disappearing. The buckles appear with a characteristic interval independent of their absolute position along the tube. This suggests the buckling is reversible, intrinsic to the nanotube and not mediated by defects. The strong correlation between tube curvature and the location of buckles confirms their role in reducing curvature-induced strain. Buckling in bent shells are well known in continuum mechanics[20] where two modes of deformation result from pure bending stresses. The Brazier effect causes the circular cross-section of the tube to become more 'ovalized' uniformly over the whole tube length[21] as the bending curvature increases. Bifurcation, on the other hand, leads to a periodic, low-amplitude rippling of the tube wall on the inside of the bend (the portion under compression). Experiment and theory show[21] that both modes often occur simultaneously, and lead to single-kink collapse as the bending moment reaches its maximum critical value. The axial

bifurcation (rippling) wavelength is given by[22]:

$$\lambda = \frac{2\pi}{(12(1-\nu^2))^{1/4}}(r_0 t)^{1/2} \approx 3.5(r_0 t)^{1/2}$$

where r_0 is the tube radius and t is the thickness of the tube wall; we have set the Poisson ratio $\nu = 0.3$ as expected for carbon nanotubes. The tube shown in Fig. 1 has a radius of 10.5 nm. If we assume that the buckles are collapsed regions with the height determined by the complete flattening[23] of the tube as constrained by the inner radius, we obtain $t = 2.6$ nm and $\lambda = 18.3$ nm. We have plotted a histogram of buckle intervals (Fig. 1d inset) and the average of the Fourier transforms (Fig. 1c, inset) for the various bent configurations. The mean value of the interval distribution (68 nm) coincides with the peak in the Fourier transform at 0.015 nm^{-1}. These values are roughly 4 times the predicted value of λ. We note two points. First, λ is for a fundamental buckling mode and modes of higher order are predicted[22]. Second, the buckling models have been developed for thin wall sections, $r_0/t \gg 10$, but in our sample $r_0/t \approx 4.0$.

Under the largest bending strains this tube buckles more severely. This is seen in the large height anomalies observed at the top right of Fig. 1a and b. The height of the nanotube to the right of the step is ~21 nm. As shown in Fig. 1f, the height of the highest buckle is almost twice the diameter of the tube. In the simplest model of a thin-walled tube collapsed into a ribbon, the width of the ribbon is πr_0. In the absence of elastic stretching of the tube wall transverse to the tube axis, this is the widest a collapsed tube can be. We have

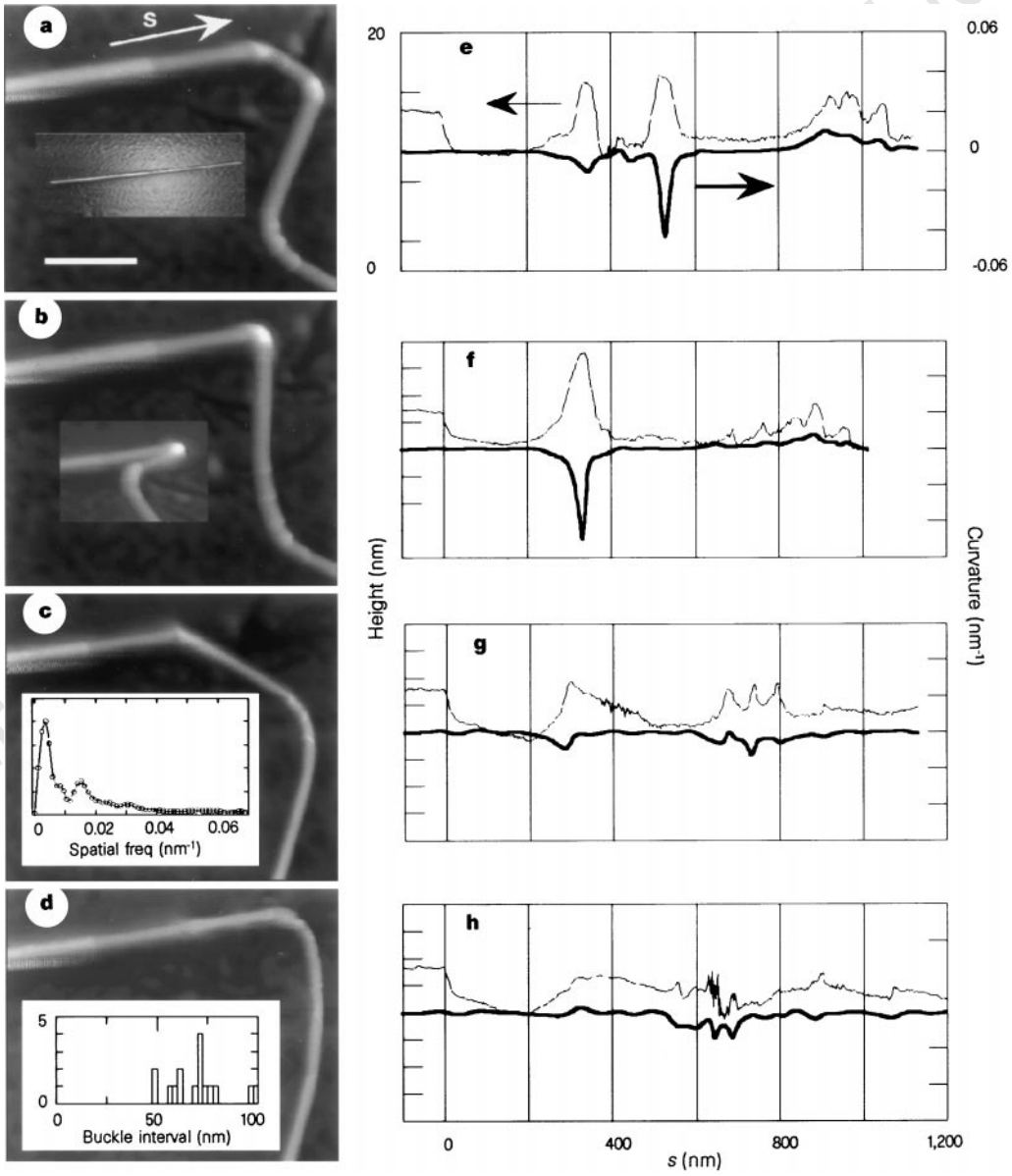

Figure 1 Curvature and height of buckles along a bent carbon nanotube. The white scale bar (in **a**) represents 300 nm and all figures are to the same scale. A 20-nm-diameter tube was manipulated (with an AFM) from its straight shape (**a** inset) into several bent configurations (**a–d**). The height and curvature of the bent tubes along its centreline (indicated by the arrow in **a**) is shown in **e–h**. The upper trace in each graph depicts the height relative to the substrate; the lower trace depicts the curvature data. Height values are relative to substrate height. The 'ripple'-like buckles occur between $s = 600$ and 1,200 nm and correspond to the tube in the lower right portion of the images in each case. We note that these buckles migrate as the tube is manipulated into different configurations. Twice during the manipulation sequence the tube is bent to ~180° (**b** inset). The appearance and disappearance of the ripple buckles, as well as the severe buckle at $s \approx 500$ nm (**e–f**), suggest elastic reversibility. The large buckle at $s \approx 325$ nm (**e**, **f**) retains its raised topographical features even after straightening (**g**, **h**), suggesting that damage has occurred at this point; but the tube does not fracture. The distance between 'ripple' buckles was determined for the various bent configurations (**a–d**). The average of the buckle interval histogram (**d**, inset) and the average of the Fourier transforms (**c** inset) for a wide range of bent configurations establish the dominant interval as 68 nm. The low-frequency peak in the Fourier transform correspond to the long-wavelength tube distortion over the entire bend region.

observed buckle heights of up to $4r_0$. This suggests that either the tube is rising up off the sample surface at these buckling points, or that the tube is rupturing and we are imaging torn sections projecting upwards. As the tube is straightened, these sections do not return to their initial height, and the unusual projections return on rebending. The radii of curvature obtained in these bends, ~20 nm (Fig. 1b inset), is the same as the diameter of the tube. It is remarkable that even though the tube sustains damage after twice bending and straightening the section, it does not separate.

Although the nanotube shown in Fig. 1 appeared to suffer permanent distortion, we have observed other cases where the nanotube survives large strains without gross damage. In Fig. 2a, a ~800-nm-long tube with $r_0 \approx 6.8$ nm was bent repeatedly to large strain with no permanent distortion of the tube topography. The left side of the tube was translated towards the top of the figure, bending the tube back on itself (Fig. 2b). The analysis of the ridge and the curvature (Fig. 2e–g) reveals behaviour distinct from the previous case. Figure 2b shows a bend with a radius of curvature (Fig. 2e) comparable to that of the large bend in Fig. 1c, but with a change in height of <3 nm. Figure 2c shows the tube with $r_c = 20\,\text{nm} \approx 3r_0$, with a change in height of 4 nm (Fig. 2f). In Fig. 2d, the tube is bent back onto itself in the other direction. This nanotube behaves very differently from the nanotube of Fig. 1 because it bends with only a single broad flattening, with no indication of periodic buckling at any curvature. The difference between the two tubes may lie in the r_0/t ratio. If we estimate the wall thickness from the tube flattening, we obtain $t = 3.25$ nm and $r_0/t = 2.1$ instead of $r_0/t = 4.0$ for the tube of Fig. 1. The height of the tube of Fig. 2 always remains within the bounds of a flattened tube, even after being bent through the sequence of curvature radii: +20 nm, +40 nm, where positive curvature has been assigned to Fig. 2b. The maximal local strain in this tube can be estimated from $\epsilon = r_0/r_c \approx 16\%$ on the outside tube surface, (r_c = radius of curvature of bend), with a corresponding compressive strain on the inner surface. The apparent lack of catastrophic damage of the tube under such large strains is remarkable. We can speculate on two ways in which the strain has been accommodated. First, it has been proposed[7] that MWNTs contain significant concentrations of defects. It might be that defects in this tube are arranged in an incoherent fashion such that they separate under tensile stress, and slide over each other reversibly under compressive stress. Second, strain might be accommodated within a severely distorted, but otherwise connected, graphene sheet. Molecular-dynamics simulations of single-walled tubes under tensile strain have shown, under certain conditions, breaking strains as large as 30% (ref. 24).

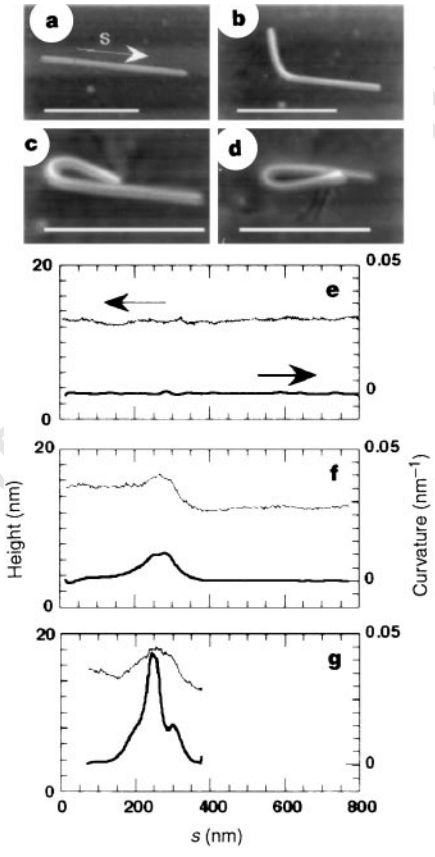

Figure 2 Carbon nanotube in highly strained configuration. The white scale bars at the bottom of each panel **a–d** represent 500 nm. **a**, The original adsorbed shape of the tube, 10.5 nm in diameter and 850 nm long. The tube is bent in steps, first upwards (**b**), until it bends all the way back onto itself (**c**). The curvature is 0.045 nm^{-1} (radius of curvature ~20 nm) which indicates the strain along the inside and outside of the tube bend is ~16%. **d**, The tube is then bent all the way back the other way onto itself, to a final curvature similar to that in **c**. Panels **e–g** correspond to **a–c** respectively, and show the height and curvature along the tube in its different configurations. This tube did show signs of irreversible damage when straightened between bends, but never 'kinked' or fractured under bending stress.

Thus carbon nanotubes are extraordinarily flexible under large strains, and resist failure under repeated bending. We have observed reversible, periodic buckling of nanotubes consistent with calculations extrapolated from continuum mechanics. Local strains as large as 16% can be sustained without separating a nanotube. In fact, we have never observed the separation of a tube by the repeated application of bending stresses. The amount of strain that we have been able to apply to a carbon nanotube has been limited by the surface forces which hold the tube in place. These results show that the carbon nanotube is a material with extraordinary strength. □

Received 6 June; accepted 5 August 1997.

1. Iijima, S. Helical microtubules of graphitic carbon. *Nature* **354,** 56–58 (1991).
2. Dresselhaus, M. S., Dresselhaus, G. & Eklund, P. C. *Science of Fullerenes and Carbon Nanotubes* (Academic, San Diego, 1996).
3. Robertson, D. H., Brenner, D. W. & Mintmire, J. W. Energetics of nanoscale graphitic tubules. *Phys. Rev. B* **45,** 12592–12595 (1992).
4. Sawada, S. & Hamada, N. Energetics of carbon nano-tubes. *Solid State Commun.* **83,** 917–919 (1992).
5. Treacy, M. M. J., Ebbesen, T. W. & Gibson, J. M. Exceptionally high Young's modulus observed for individual carbon nanotubes. *Nature* **381,** 678–680 (1996).
6. Dai, H., Hafner, J. H., Rinzler, A. G., Colbert, D. T. & Smalley, R. E. Nanotubes as nanoprobes in scanning probe microscopy. *Nature* **384,** 147–150 (1996).
7. Zhou, O. *et al.* Defects in carbon nanostructures. *Science* **263,** 1744–1747 (1994).
8. Lieber, C. Nanotube derived materials. *Bull. Am. Phys. Soc.* **42,** 591 (1997).
9. Yakobson, B. I., Brabec, C. J. & Bernholc, J. Nanomechanics of carbon tubes: instabilities beyond the linear response. *Phys. Rev. Lett.* **76,** 2511–2514 (1996).
10. Ruoff, R. S. & Lorents, D. C. Mechanical and thermal properties of carbon nanotubes. *Carbon* **33,** 925–929 (1995).
11. Despres, J. F., Daguerre, D. & Lafdi, K. Flexibility of graphene layers in carbon nanotubes. *Carbon* **33,** 87–92 (1995).
12. Iijima, S., Brabec, A., Maiti, A. & Bernholc, J. Structural flexibility of carbon nanotubes. *J. Chem. Phys.* **104,** 2089–2092 (1996).
13. Ebbesen, T. W., in *Carbon Nanotubes: Preparation and Properties* (ed. Ebbesen, T. W.) 225–248 (CRC, Boca Raton, 1997).
14. Ruoff, R. S. & Kadish, K. M. *Fullerenes; Recent Advances in the Chemistry and Physics of Fullerenes and Related Materials* Vol. 2 (Electrochem. Soc., Pennington, NJ, 1995).
15. Ebbesen, T. W. & Ajayan, P. M. Large scale synthesis of carbon nanotubes. *Nature* **358,** 220–222 (1992).
16. Taylor, R. M. II *et al. The Nanomanipulator: A Virtual Reality Interface for a Scanning Tunneling Microscope.* (ed. J. T. Kajiya) 127–134 (Association for Computing Machinery, New York, 1993).
17. Finch, M. *et al. Surface Modification Tools in a Virtual Environment Interface to a Scanning Probe Microscope.* (ed. P. Hanrahan & J. Winget) 13–18 (Association for Computing Machinery, New York, 1995).
18. Pizer, S. M., Eberly, D., Morse, B. S. & Fritsch, D. S. Zoom-invariant vision of figural shape: the mathematics of cores. *Comput. Vision Image Understand.* (in the press).
19. Fritsch, D. S., Eberly, D., Pizer, S. M. & McAuliffe, M. J. Simulated cores and their applictaions in medical imaging. *Information Processing in Medical Imaging, Proc. IPMI '95* (ed. Y Bazals, C. Barillot and R. Di Paola) 365–368 (Kluwer, Dordrecht, The Netherlands (1994).
20. Landau, L. D. & Lifshitz, E. M. *Theory of Elasticity* (Pergamon, Oxford, 1986).
21. Ju, G. T. & Kyriakides, S. Bifurcation and localization instabilities in cylindrical shells under bending – II. Predictions. *Int. J. Solids Structures* **29,** 1143–1171 (1992).
22. Axelrad, E. L. On local buckling of thin shells. *Int. J. Non-Linear Mech.* **20,** 249–259 (1985).
23. Chopra, N. G. *et al.* Fully collapsed carbon nanotubes. *Nature* **377,** 135–138 (1995).
24. Yakobson, B. I., Campbell, M. P., Brabec, C. J. & Bernholc, J. High strain rate fracture, and C-chain unraveling in carbon nanotubes. *Comput. Mater. Sci.* **8,** 341–348 (1997).
25. Lu, J. P. Elastic properties of carbon nanotubes and nanoropes *Phys. Rev. Lett.* **79,** 1297–1300 (1997).

Acknowledgements. We thank O. Zhou for providing the carbon nanotube soot and S. Paulson for help with sample preparation. This work was supported by the National Science Foundation, National Institutes of Health National Centers for Research Resources, Topometrix, Inc. and Silicon Graphics, Inc.

Correspondence and requests for materials should be addressed to R.S. (e-mail: rsuper@physics.unc.edu).